A Reactive Force Field for Simulations of the Pyrolysis of Polysiloxanes into Silicon Oxycarbide Ceramics

Ilia Ponomarev[1], Adri C. T. van Duin[2], and Peter Kroll[1,*]

[1]Department of Chemistry and Biochemistry, The University of Texas at Arlington

[2]Department of Mechanical and Nuclear Engineering, Pennsylvania State University

700 Planetarium Place, Arlington, Texas 76019, United States.

*pkroll@uta.edu

Abstract

We provide a new Reactive Force Field (ReaxFF) for simulations of silicon oxycarbide (SiCO) ceramics and of their syntheses from inorganic polymer precursors. The validity of the force field is extensively tested against experimental and computational thermochemical data. Its performance in simulation at elevated temperature is gauged by results of comprehensive ab-initio molecular dynamic simulations. We apply the force field to the formation of amorphous SiCO in a simulated polymer pyrolysis. Modeling results are in good agreement with experimental observations and allow new insight into the formation of graphene segregations embedded in an amorphous oxycarbide matrix. The new reactive force field for Si-C-O-H compounds enables large-scale and long-time atomistic simulations with unprecedented fidelity.

1. Introduction

Silicon oxycarbide (SiCO) materials possess a wide range of attractive properties such as chemical durability[1], high-temperature stability[2], high creep-resistance and other specific mechanical properties[3-4]. SiCO materials are used or proposed to be used in applications for gas separation[5-6], thermal protection [7], radiation protection[8-9], advanced drug delivery[10], low-κ dielectric electronics[11], and energy storage[12]. Synthesis of SiCO proceeds via "bottom-up" processes: sol-gel syntheses[13], polymer-to-ceramic routes[14], and different flavors of vapor deposition methods.[15-17]

Composition and structure of SiCO materials depend on the involved chemistry, details of the processing and, not at least, on the thermal history of the material. Synthesized at temperatures below 1200°C the material remains amorphous, and crystallization occurs only at significantly higher temperatures[18]. Even in the amorphous state significant differences exists. For instance, low-κ SiCO thin films for electronic application contain significant amounts of hydrogen and methyl groups[19]. Here we focus on carbon-rich SiCO ceramic materials produced by the polymer-to-ceramic route. These ceramics exhibit a "SiCO glass" phase with so-called "free" carbon embedded in the matrix[14]:

$$SiC_{x+y}O_{2(1-x)} = \{x \cdot SiC + (1-x)SiO_2\} + y \cdot C_{free}$$

The SiCO glass, a stoichiometric mixture of SiO_2 and SiC, comprises a random network of Si-O and Si-C bonds forming mixed SiC_nO_{4-n}-tetrahedra. [18, 20-21] Carbon within the glass appears ("carbidic") in CSi_4 tetrahedra like in SiC, while O atoms bridge between Si atoms as in silica glass. The "free" carbon phase expresses similar to graphite or graphene[22]. Stoichiometric SiCO glass without "free" carbon can be synthesized[3]. The morphology of the "free" carbon, its interface to the glass matrix as well as the amount of hydrogen remaining in the material are hotly debated issues in concurrent research[23-24].

Atomistic modeling and accurate Density Functional Theory (DFT) calculations have contributed to better understanding local structures in SiCO materials. The SiCO glass has been characterized early on[25] and various interfaces between SiCO and "free" carbon have been studied.[26] Combining computational and experimental ^{29}Si NMR illuminated bonding at interfaces in amorphous SiCO.[21] Unfortunately, DFT calculations are computationally very expensive, which limits model sizes to a few hundred atoms and simulation times to below one nanosecond. Through empirical potential simulations, on the other side, it is feasible to explore mechanical properties of SiCO in models with millions of atoms extending several nm[27]. However, these models lack accuracy of chemical bonding, proper atomic environments, and acceptable thermochemistry.

The reactive force field (ReaxFF)[28] bridges the gap between accurate DFT simulations and empirical potential simulations. It achieves a level of accuracy approaching DFT simulations for a wide set of molecular reactions in gas phase[28] and on surfaces[29-30]. At the same time ReaxFF is several orders of magnitude less computationally expensive, which allows modeling chemical processes in larger systems for longer simulation times as compared to DFT simulations. A few studies of modeling reactive processes in SiCO using ReaxFF have been published recently[31-33]. As we will show further below, the Newsome et al[31] ReaxFF parameterization used in these studies as well as Soria et al[29] parameterization developed later fail to model many distinct features of SiCO and resulting structures are inadequate. Thus, to achieve the desired level of fidelity for a wide range of local atomic configurations it requires careful development of the numerous parameters describing interaction.

Here we represent new ReaxFF parameters describing interactions among Si, C, O, and H atoms in SiCOH materials. Starting with an existing ReaxFF parameterization[31], we take advantage of data of several thousands of DFT-computed models of SiCO and involve a self-learning process to eliminate pitfalls and traps. The new reactive force field

is then applied to simulate the polymer-to-ceramic conversion of a cross-linked polysiloxane precursor.

2. Computational methods

The reactive force field (ReaxFF) has been designed to model chemical reaction through molecular dynamics simulations[28]. Guided by quantum chemical calculation, the energy of a system is partitioned into a variety of terms, including two-center covalent bond energy, Coulomb interactions, van der Waals interactions, a description for under- and over-coordination of atoms, angular and torsional terms, additional bond conjugation and penalties. A detailed description is given in the Reference [[28]]. A typical parameter set comprises 39 general parameters, another 32 parameters per atom and 16 parameters per bond, plus 7 additional off-diagonal bond parameters for heteroatomic bonds, 7 angular parameters, 5 torsion parameters and 4 parameters to describe hydrogen bonding. With more than 100 parameters to describe a system such as polysiloxane and SiCO ceramics, the chance of over-parameterization is immanent. Therefore, deriving a high-fidelity parameter set requires careful optimization against quality data, either experimental or computed via quantum mechanics (QM) methods.

We started with an existing parameters set for SiCO developed by Newsome et al.[31] This force field was developed with the purpose to model oxidation of silicon carbide. It incorporates essential thermochemistry of the Si-C-O system, including enthalpies of formation of SiC and SiO_2, reaction enthalpies of carbothermal reduction of SiO_2, and enthalpies of formation for a variety of small molecules. We then added recent force field parameters by Srinivasan[34] for the description of carbon-carbon interactions. Thereafter, we provided structure and energy data from our library of DFT-optimized SiCO models. The library comprises over 10000 hypothetical crystalline SiCO structures[35] and more than 1000 models of amorphous SiCO generated via a network algorithm or through melt-quench ab initio molecular dynamics simulations.[21, 25-26, 36-37]

Using the accumulated data we optimized force field parameters for SiCOH within the ReaxFF software[28]. At this stage we achieved mapping of DFT energy differences to ReaxFF energy differences. However, the reverse mapping lacked strong correlation. Consequently, we augmented the training set with $SiC_xO_yH_z$ models created by ReaxFF itself via melt-quench simulations and subsequently optimized in DFT. This recursive learning strategy expanded the range of configurations explored and enabled the development of robust force field parameters.

The Density Functional Theory[38] calculations in this work are carried out with the Vienna Ab Initio Simulation (VASP) package[39-40]. We use the Projector Augmented Wave (PAW)[41-42] method and approximate electron exchange and correlation by the Perdew-Burke-Ernzerhoff (PBE) generalized gradient approximation (GGA)[43-44]. The DFT-D2 method of Grimme[45] is applied to account for van der Waals interactions. The energy cutoff for the expansion of the wave function into the plane-wave basis is 500 eV. Ab-initio molecular dynamic simulations are performed at reduced energy cutoff under constant volume with a time step of 1 fs.

Molecular dynamics (MD) simulations with ReaxFF are performed with the Large-scale Atomic/Molecular Massively Parallel Simulator (LAMMPS) software[46] distributed by Sandia National Laboratories and its reax/c user's package[47]. We apply the Bussi-Donadio-Parrinello thermostat (temp/csvr command)[48] for temperature control. Depending on the hydrogen content of the model we use a time step of 0.1 fs to 1.0 fs for the integration of the equations of motion.

3. Force Field development

Challenges calling/identifying the need for a new Force Field

A proper Si-C-O-H force field must provide accurate description of the stoichiometric silicon oxycarbide glass phase that develops during synthesis of SiCO ceramics[3, 13-14, 18], but also occurs at reaction fronts during oxidation of SiC[49-50]. A fundamental

characteristic of the SiCO glass are SiC_nO_{4-n} tetrahedra[18, 20]. These so-called mixed tetrahedra emerge in the glass phase of sol-gel processed or polymer-derived SiCO ceramics[51], but also develop upon oxidation of SiC (starting with only SiC_4-tetrahadra). Unfortunately, the parameter sets developed by Newsome et al. and Soria et al. cannot properly describe mixed SiC_nO_{4-n} tetrahedra, as we show in Figure 1. While both parameterizations share the same issues, we focus our comparison on the parameter set of Newsome et al., since we used this as the starting point for our work. A perfect network of SiCO glass previously optimized using DFT is severely distorted in a MD simulation at 300K using Newsome et al. parameters. The force filed ruptures several Si-C bonds in mixed SiC_nO_{4-n} tetrahedral units, creating defects such as under- and over-coordinated sites.

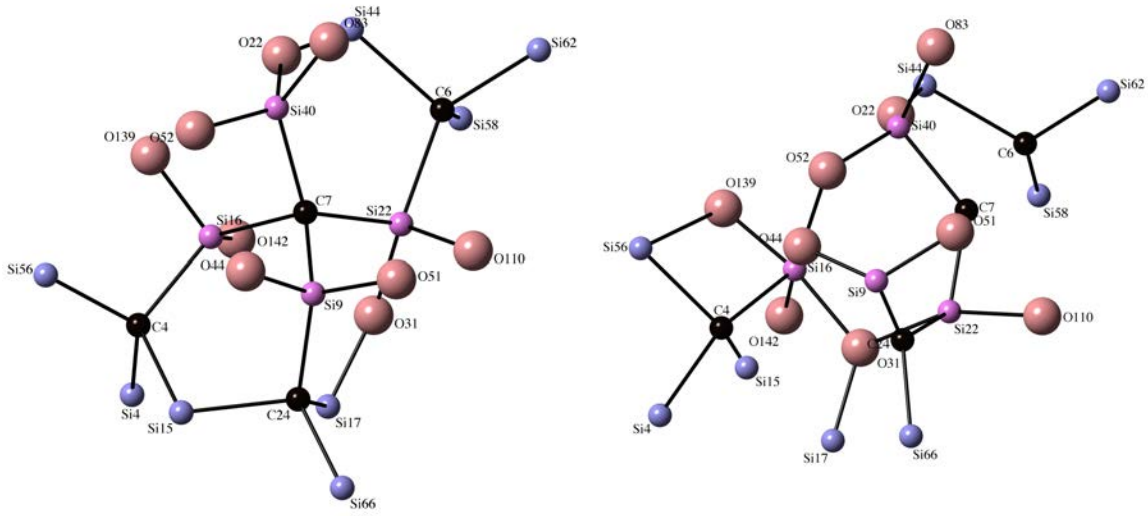

Figure 1. A fragment of the model of stoichiometric SiCO glass (composition $Si_{104}C_{24}O_{160}$) before (left) and after (right) 100 ps long MD simulation at 300K using Newsome ReaxFF parameters. We emphasize four mixed SiC_nO_{4-n} tetrahedral (Si in magenta) bonding to C (label C7). Sphere represent atoms: C (black), Si (blue and magenta), O (red).

We find another deficiency of the existing parameters by comparing ReaxFF energies with those calculated by DFT for stoichiometric SiCO glass models. This is shown in detail further below, when we highlight the performance of the new set of parameters we developed. Finally, the parameter set of Newsome et al. does not catch properly the remarkable kinetic stability of stoichiometric SiCO glass. Network models of glass SiCO are kinetically stable in ab-initio molecular dynamic simulations (aiMD) at elevated temperatures, for example at 2600K for 20 ps and longer[25]. The aiMD simulations show "melting" (i.e. breaking of bonds) only at higher temperatures. In sharp contrast, a ReaxFF MD simulation using the parameter set of Newsome et al. significantly deteriorates the model already at 1200K, a temperature at which a-SiCO remains stable in the experiment. Simulation at 2000K ruptures the model completely and leaves none of the existing carbidic carbon units, CSi_4-tetrahedra, intact, see Figure 2. The formation of C-C and C-O bonds in the simulation goes along with under-coordination of Si and formation of Si-Si bonds in the final model.

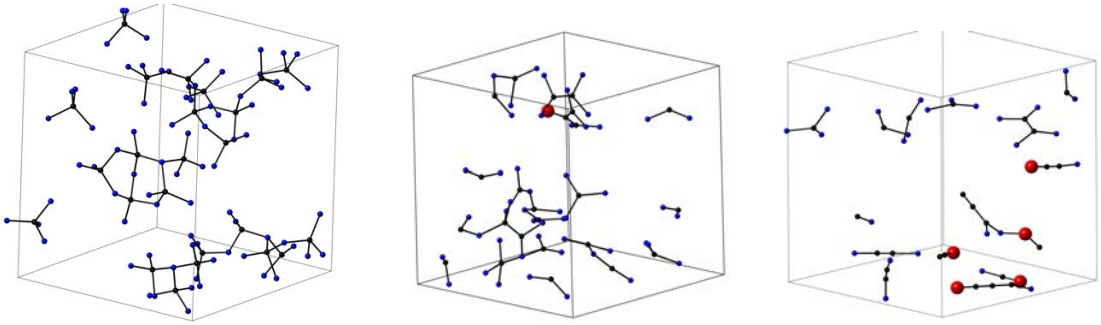

Figure 2. A model of stoichiometric SiCO glass (composition $Si_{104}C_{24}O_{160}$) before (left) and after 100 ps long MD simulation at 1200K (center) and 2000K (right) using Newsome ReaxFF parameters. Only C atoms and their nearest neighbors are displayed.

Deficiencies of the Newsome parameters have recently been identified by Takamoto et al. as well[52]. Their study underlines the call for developing a new set of parameters for

ReaxFF which can properly handle the variety of Si-C-O interactions occurring in polysiloxanes and silicon oxycarbide ceramics.

Performance of the newly developed force field

Part 1a: stoichiometric SiCO models: energy

The significant improvement of correspondence between DFT-computed energies and ReaxFF energies using the new parameter set is shown in Figure 4. We compare DFT computed energies for a standard set[25] of network models with composition $Si_{48}C_{16}O_{64}$ with energies computed by ReaxFF. In comparison with the previous force field, the new developed force field parameters UTA1 yield almost a unit slope, indicating that energy differences in DFT agree with those in ReaxFF. While the graph displays the relation for models with composition $Si_{48}C_{16}O_{64}$ only, we obtain equivalent agreement for all other stoichiometric compositions as well.

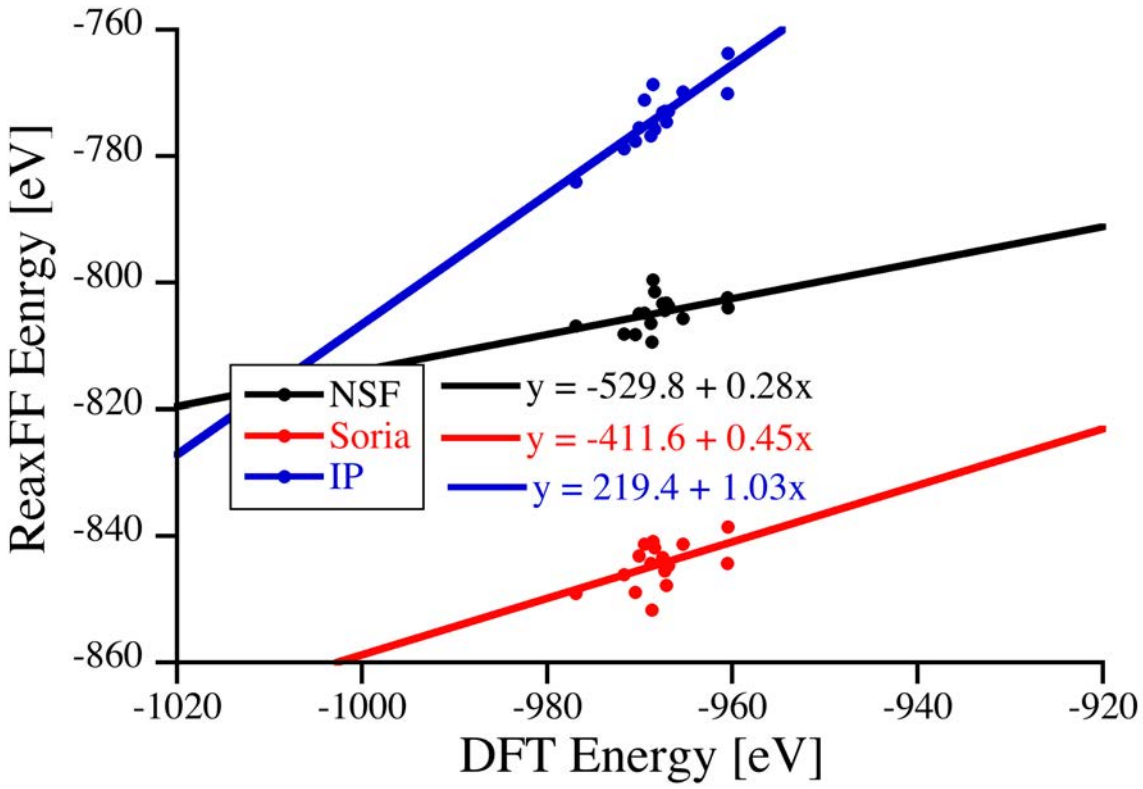

Figure 3. Comparison of DFT-energies of stoichiometric SiCO glass models with composition $Si_{48}C_{16}O_{64}$ with ReaxFF energies using parameters of Newsome et al.[31], Soria et al.[29], and UTA1 ReaxFF parameters.

Part 1b: dynamic evolution of stoichiometric SiCO models

Besides achieving correspondence of energy differences, we also improve dynamic stability of SiCO glass structures. We performed MD simulations of stoichiometric SiCO with composition $Si_{104}C_{24}O_{160}$ ($24{\cdot}SiC+80{\cdot}SiO_2$, 24 mol-% SiC) using two different sets of models, each comprising three independent structures. One cohort exhibits a random distribution of mixed SiC_nO_{4-n}–tetrahedral. This is typical for SiCO glass synthesized at about 1000 °C[2, 18, 53]. Models in the second set are "segregated", with preference of SiC_4- and SiO_4-tetrahedra on the cost of mixed units. One structure even exhibits a large SiC-nucleus embedded by SiO_2. Such configurations are typical for the partitioned yet still disordered state of SiCO materials annealed to higher temperatures (1200°C)[18]. They also occur at the interface between silicon carbide and its natural oxide, silica. After heating to 2000K and annealing at this temperature for 100 ps, we analyzed all structures. We focus on persistence and stability of (carbidic) C atoms within CSi_4-tetrahedra and of mixed SiC_nO_{4-n}–tetrahedra. Figure 4 displays one of the "random" a-SiCO models before and after completed simulation. Structural information on the models is summarized in Tables 1 and 2.

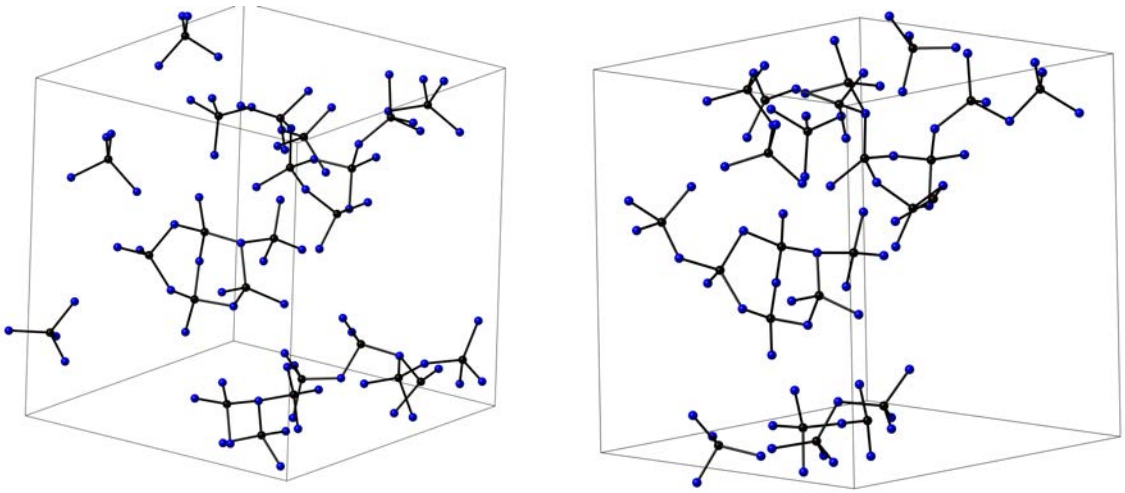

Figure 4. A model of stoichiometric SiCO glass (composition $Si_{104}C_{24}O_{160}$) before (left) and after (right) 100 ps long MD simulation at 2000K using the UTA1 ReaxFF parameters set. Only C atoms and their nearest neighbors are displayed.

Table 1. Amount (in %) of carbidic C atoms in $Si_{104}C_{24}O_{160}$ retaining tetrahedral coordination (CSi_4) after 100 ps simulation at 2000K.

Models	NSF	Soria	UTA1
Random	3	22	83
Segregated	4	17	96
All models	3	26	90

Table 2. Amount (in %) of unchanged SiC_nO_{4-n}–tetrahedral in $Si_{104}C_{24}O_{160}$ after 100 ps simulation at 2000K.

Si unit	NSF		Soria		UTA1	
	Random	Segregated	Random	Segregated	Random	Segregated
SiO_4	0	1	25	40	76	70
SiO_3C	0	0	6	10	76	67
SiO_2C_2	0	0	0	0	62	82
$SiOC_3$	0	0	0	3	82	86
SiC_4		0		0		95
All units	0		18		74	

Overall, the new force field provides stability of carbidic carbon at elevated temperatures and retains most of the mixed SiC_nO_{4-n}–tetrahedral environments. This will be important

for modeling phase separation in SiCO, which involves formation of SiC nuclei. Moreover, it is essential for the simulation of pyrolysis of polymer precursors, for example of poly-methyl-siloxanes. Those encounter a Kumada-like rearrangement[54] as their most critical step[14]. Thermal activation leads to the cleavage of Si–O bonds and insertion of carbon forming Si–C bonds in the polymer backbone. This process yields the random distribution of mixed SiC_nO_{4-n}-tetrahedra, even if the molecular or polymeric precursors have a singular distinct environment only[18, 55].

Part 1c: modeling SiO_2 glass

Besides providing description of SiCO glass, our ReaxFF parameterization is also suitable to model pure SiO_2 glass. We performed melt-quench simulations to generate amorphous SiO_2 models. Starting with a 1032 atom model at 4000K, we quenched the system with a rate of 5 K/ps. Throughout the simulation we maintained a NPT ensemble, allowing the density of a-SiO_2 to adjust. A brief analysis of structural parameters of a-SiO_2 model is given in Table 3, and compared with data from models generated similarly using the parameters of Newsome et al.[31] We also include results obtained using yet another set of ReaxFF parameters especially designed for modeling a-SiO_2[56-57]. Our new ReaxFF parameters yield less than 5% of defects such as under- or over-coordinated Si and O atoms. Density, average Si-O bond length and average Si-O-Si bond angle are close to the experimental values. Overall, our model compares well to structures obtained using a parameterization of ReaxFF developed especially for silicates[56-57].

Table 3. Structural parameters of SiO_2 models (1032 atoms) generated via melt-quench using ReaxFF with original Newsome parameters[31] (NSF), Pitman parameters[56-57] and the parameters presented in this work (IP).

Force field	ρ [g/cm^3]	Number of atoms per model adopting coordination				Number of bonds per model		Average	
		Si[3]	Si[5]	O[1]	O[3]	Si-Si	O-O	d_{Si-O} [Å]	<Si-O-Si> [°]
NSF	2.52	1	22	15	37	0	4	1.60	148

UTA1	2.17	13	9	13	9	1	2	1.62	146
Pitman	2.10	9	10	6	7	0	2	1.64	138

Part 1d: inclusion of "free" C into SiCO

The "free" carbon phase is characteristic of most silicon oxycarbide ceramics. Its genesis during synthesis and processing is the focus of many investigations, and tailoring its emergence through the molecular of polymer structure is a key issue for synthesis. Indeed, the development of the interface between glass matrix and "free" carbon is still an unresolved topic. A library of SiCO models comprising "free" carbon has been part of the parameter development[21, 26]. Here we show the performance of the new ReaxFF parameter set for the generation of SiCO structures via melt-quench MD simulations. 20 models of composition $Si_5CO_8+10C_{free}$, each comprising 120 atoms and a density of 2.2 g/cm^3, were generated via melt-quench simulations using a cooling rate of 20 K/ps. The models were finally optimized within ReaxFF. Subsequently, we switched to DFT calculations for direct comparison between ReaxFF energies and DFT energies. We computed the energy of each model at the beginning and the end of its DFT optimization. The difference between the two energies is a measure of "proximity" of potential energy surfaces of ReaxFF and DFT. Figure 5 provides a comparison for different compositions, with and without free carbon, generated within ReaxFF and further optimized in DFT.

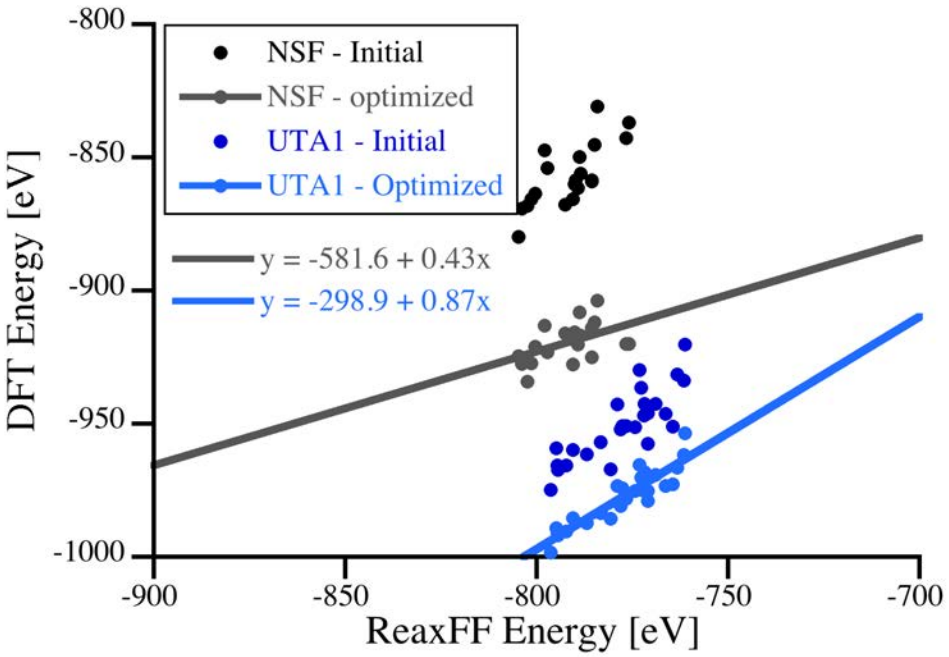

Figure 5. Energies of the models $Si_5CO_8+10C_{free}$ (ρ = 2.2 g/cm^3) generated via ReaxFF melt-quench simulation and optimized in DFT. "Initial" – first energy computed via DFT. "Optimized" – final DFT energy. NSF – original Newsome force field[31], UTA1 – force field parameters developed in this work.

Structures generated with the new parameter set come out much closer to the DFT optimized state than models generated with parameters of Newsome et al.. The average energy gained during DFT optimization (0.22 eV/atom compared to 0.69) is much lower for the new than for the previous parameter set. Although we do not obtain perfect agreement, the new ReaxFF parameters set generates models very similar to those we obtain via DFT melt-quench simulations. Figure 6 shows a comparison between models generates via ab-initio and ReaxFF melt-quench MD simulations for the composition $Si_5CO_8+10C_{free}$ with the initial density of 2.2 g/cm^3. Both models comprise a layer of "SiCO glass" sandwiched between a buckled graphene layers of "free carbon" phase.

Note that size, periodic boundary conditions and composition have a major impact on the final structure. Nevertheless, the resemblance of both models is striking.

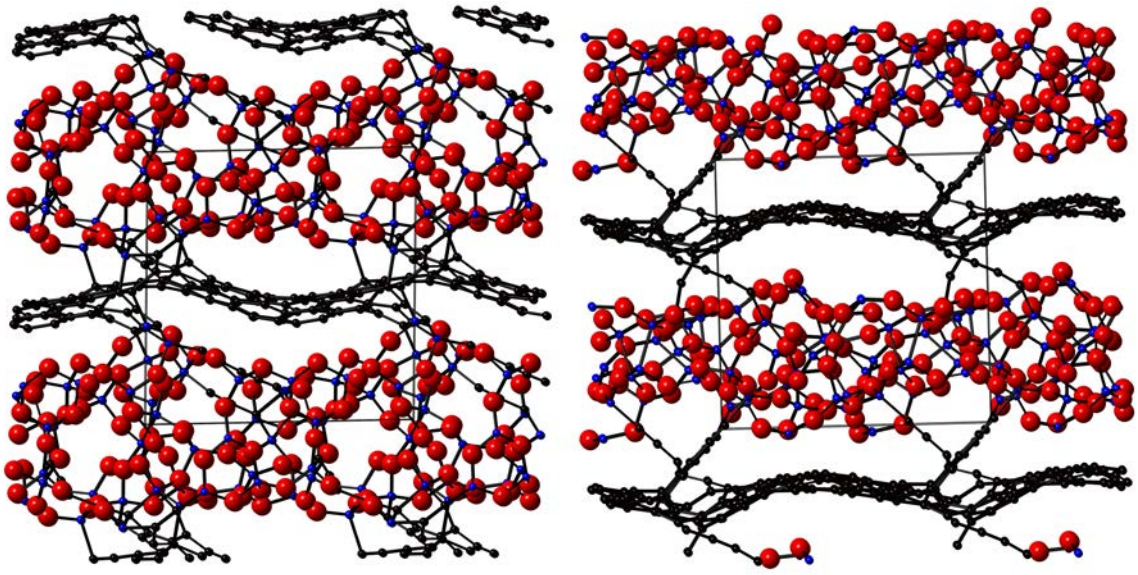

Figure 6. Amorphous models [left: DFT; right: ReaxFF using UTA1 parameters] of Si_5CO_8+$10C_{free}$ (192 atoms) generated via melt-quench MD simulation with a cooling rate of 12.5 K/ps starting from 5000K.

Part 1e: inclusion of hydrogen

Silicon oxycarbide ceramics are produced by pyrolysis of molecular or polymeric precursors that contain substantial amounts of hydrogen.[13-14] Presence and content of hydrogen plays significant part in carbon segregation[32], electric properties of the final material[15], or withstanding radiation damage by a-SiCO(:H)[8]. We included parameters for the interaction between H and the other elements, C, O, and Si from Newsome et al[31]. Some modifications were necessary to avoid unphysical bonding situations, and once again we located optimum parameter through repeating learning cycles of model generation and DFT optimization. Results for SiCOH models are quite similar to what has been shown before (e.g. Figure 5). Here we support "robustness" and "proximity" of ReaxFF and DFT energy minima in yet another way. We first generated a model of

composition $Si_{25}C_{55}O_{40}H_{12}$ via melt-quench MD simulation (cooling rate 25 K/ps) in ReaxFF. Thereafter we started a cycle of optimizations first using ReaxFF then using DFT. After the first DFT optimization we keep the volume of the model constant. The cycle was the repeated several times. If potential energy surfaces of ReaxFF and DFT would not correspond well to each other, this cycling would produce more and more different structures. This happens, indeed, if "cycling" is done using a Tersoff-potential with parameters taken from Ref[58-61] and DFT. Using ReaxFF parameters of Newsome et al. and performing "cycling" creates many diverging structures as well. With the new parameter set, on the other side, models converge back to almost identical positions in every cycle. The sequence of energies of optimized structures is shown in Figure 7. We followed the same process also with a second model generated first using ab-initio melt quench simulations in DFT, and performed repeatedly optimizations in DFT followed by optimizations using ReaxFF. Here too, models converge back to almost the initial positions after every cycle.

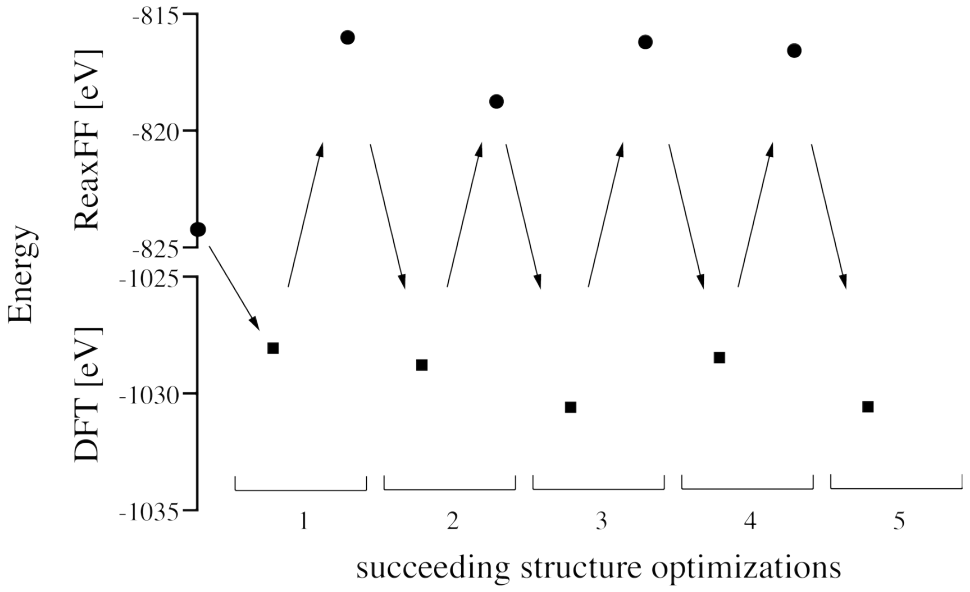

Figure 7. Final energies in repeated optimizations of SiCOH model (composition $Si_{25}C_{55}O_{40}H_{12}$) within DFT and ReaxFF.

Part 1f: summary of accomplishments

Before we go on and apply the new force field to model chemical processes, we can summarize the accomplishments of the parameter development. The new force field has been adjusted to provide a mapping of DFT energy differences to ReaxFF energy differences. For a variety of SiCO models, including those with "free" carbon, we show that energy differences agree on average. Moreover, modeling structures within ReaxFF and subsequently optimizing them in DFT shows that the reverse mapping holds as well. Thus, ReaxFF simulations of SiCO do not provide artificial structures that are local minima only with respect to the reactive force field. Those situations have been eliminated by the extensive learning strategy, repeatedly using results of ReaxFF simulations as test models for the development process.

Despite the obvious progress, our current set of ReaxFF parameters for SiCO is not perfect. For instance, we notice higher tolerance of ReaxFF for three-coordinated Si[3] and O[3] species. Those rarely appear in DFT-generated models of SiCO, and reactivity of Si[3] is well-known in experiments[62]. We also notice that modeling SiCO by ReaxFF yields a discernible preference for density of SiCO depending on composition. Simulations at constant volume show clear dependence of energy on density. On the other side, this dependency is much weaker when using network modeling or ab-initio MD simulations at constant volume to model SiCO[25]. Such remaining imperfections will be addressed in future work. With the new ReaxFF parameters at hand we can advance to the simulations of SiCO formation via thermal treatment of polymer precursors.

Part 2. Modeling the polymer-to-ceramic conversion: pyrolysis and annealing of PHMS-DVB

Providing deeper insight into processing of polymers into ceramics is essential for tailoring materials properties and for developing optimized chemical precursors. Quantum-chemical calculations provide accurate simulations, but unfortunately hit barriers associated with size and time. Simple (semi-) empirical potentials (e.g. Tersoff[63])

on the other side lack accuracy (and ability) in the description of chemical reactions and processes. This is where the reactive force field finds its application: tuned to accurate quantum-chemical calculations with the benefits of scalability of empirical simulations. As an example of a polymer-to-ceramic conversion, we model the pyrolysis of polymethylhydridosiloxane (PMHS) cross-linked with divinylbenzene (DVB).[64] This polymeric precursor has been used for synthesis of bulk and porous SiCO ceramics.[65-66] Ceramics obtained after pyrolysis are well characterized and comprise an amorphous SiCO phase with high "free" carbon content.[66] Materials synthesized from PMHS and DVB have been investigated as Li-anode material[67-68], for environmental remediation[24], sensors[69], gas separation[6], and as molecular sieves[24].

We start our simulation with modeling a cross-linked PMHS/DVB polymer, connecting different strands of PMHS with DVB. Figure 8 (left) shows a fragment of the structure. Note that the ratio of polymer units [-Si(H,Me)-O-] to double bonds [-H_2C=CH-] of DVB vinyl group is 2:1. This corresponds to a mass ratio of 4:1 between PMHS polymer units and molecular DVB. Essentially, it leaves every other Si-H bond available for further reactions. The fragment shown in Figure 8 is then interpenetrated by a second similar cross-linked polymer, yielding an entangled three-dimensional polysiloxane, as shown in Figure 8 (right). The model is replicated in all three directions and placed into a rectangular box with dimensions of approximately 4.0 x4.5x4.0 nm^3 under periodic boundaries. The composition is $Si_{512}C_{1792}O_{512}H_{3328}$ (6144 atoms) with a density of 1.08 g/cm^3. This polymer model serves as starting configuration for further simulations.

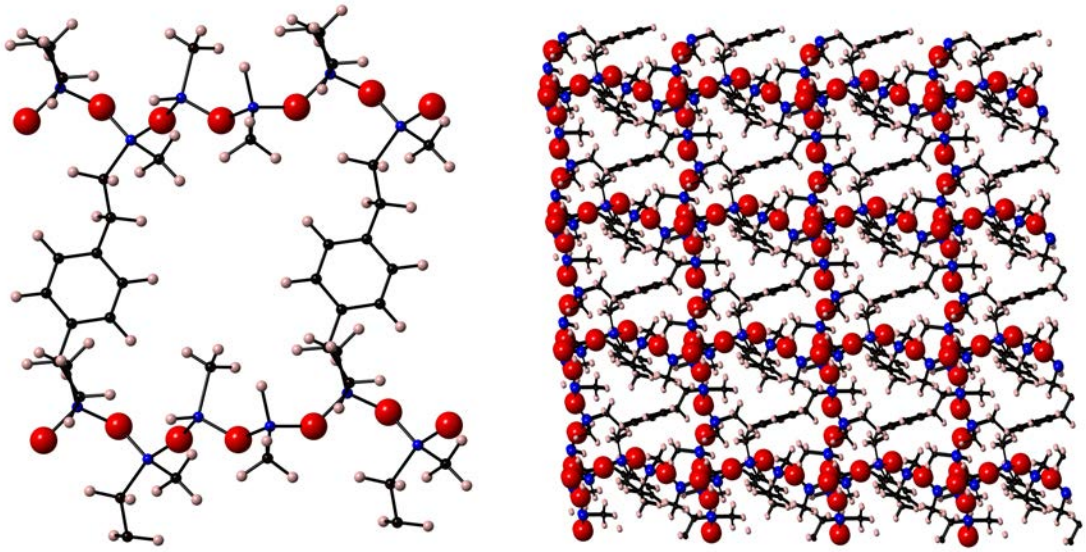

Figure 8. Left - fragment of the PHMS-DVB polymer structure. Right – entangled 3D polymer structure. Spheres are Si (blue), C (black), O (red), H (pink).

After an initial equilibration at room temperature, we heat the model to 2500K at constant volume with the rate of 25 K/ps. This process is required to observe reactions within feasible simulation times[70]. Experimental processing conducts the pyrolysis with heating rates of 5 K/min to temperatures between 900 ºC and 1200 ºC[14, 67] Once the maximum temperature is reached, we anneal the system for 1 ns ($5 \cdot 10^6$ time steps using Δt=0.2 fs). Throughout the annealing we maintain a constant pressure of 2000 bar to prevent "foaming" of the model. We also monitor the formation of gaseous reaction products, H_2, CO, CO_2, H_2O, O_2, CH_2O, C_2H_2, C_2H_4. Every 5 ps we remove persistent gas molecules. This process effectively simulates the evolution of gaseous species as monitored by mass-spectrometry[71]. Finally, we cool the system down to 0K while continuing removal of gaseous species as they appear. In Figure 9 we display the temperature profile for the simulation together with the evolution of composition of the system.

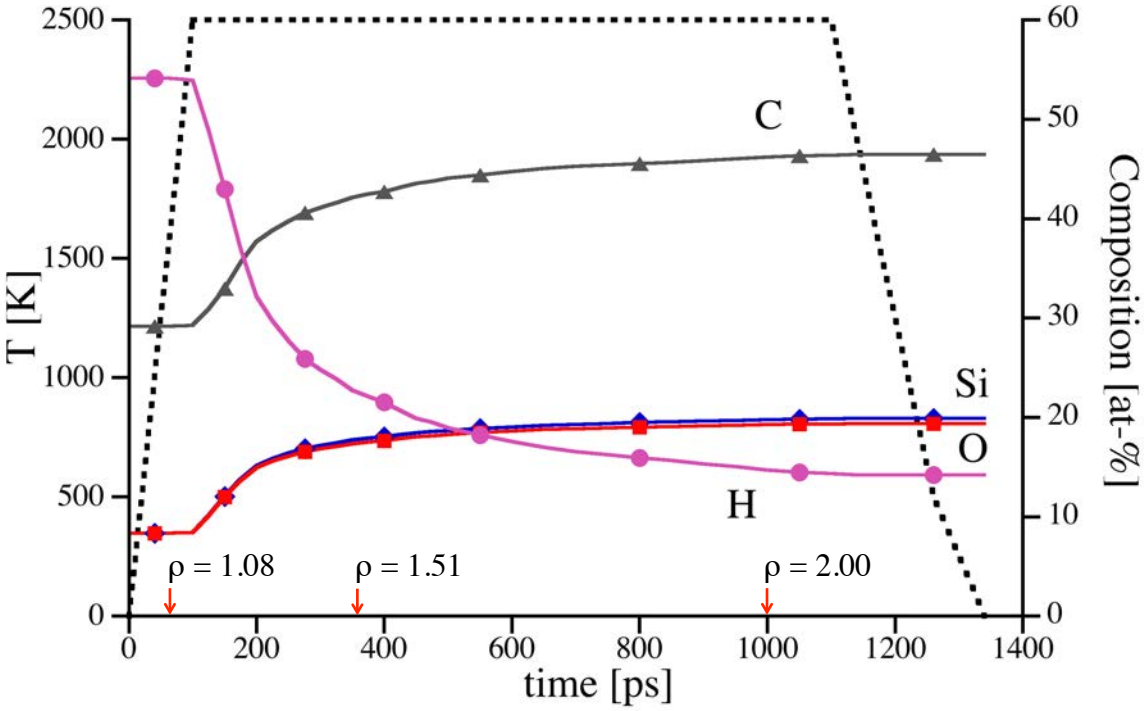

Figure 9. Time-temperature scheme (black dotted line) of simulated annealing of PMHS-DVB polymer. The second y-axis refers to the composition of the model (in atom-%) as a function of annealing time. Density (in g/cm^3) milestones are marked with arrows on x-axis.

Details of the chemical process will be given elsewhere. In brief, first processes we observe are H and CH_3-groups forming gaseous CH_4, leaving behind under-coordinated Si. These quickly react in various ways, creating Si-Si bonds, forming three-coordinated O, or terminating by H. With increasing temperature, the polymer -Si-O- backbone becomes flexible enough to allow insertion of methyl groups into the polymer chain (Kumada-like rearrangement). Only very few CO molecules develop, and the Si:O ratio is almost maintained throughout the simulation. At the same time, DVB units dissociate leaving behind vinyl-fragments and phenyl-rings. The latter then start to form larger agglomerates like poly-aromatic carbon. The latter process is facilitated by the openness of the polymer backbone, which allows large windows to appear in the structure suitable

for the migration of larger carbon units. Ultimately, we observe segregation of tubular carbon and SiCO glass (Figure 10). At this stage of the simulation, mass loss happens through removal of H_2 only.

Table 6. Annealing of PMHS-DVB polymer precursor with PMHS:DVB mass ratio of 2:1 – computations vs. experiment. "C_{free}" represents mass-% of continuous C structure, not attached to Si.

Property	ρ [g/cm^3]	Mass loss [%]	Composition [mass-%]				
			Si	C	O	H	C_{free}
Simulation	2.02	22.6	39.2	38.1	21.8	0.9	32.8
Experiment[4, 51, 72]	1.95	23	38.1	40.3	21.3	0.3	32

Composition and density of models obtained, averaged over 2 simulations, are summarized in Table 6 and compared with experimental results[4, 51, 72]. Mass loss and final density matches experimental data auspiciously. In the course of the simulations the linear dimensions of the model shrink by 25%. The final structure of a-SiCO ceramic produced by simulated pyrolysis of a PMHS/DVB polymer is shown in Figure 10.

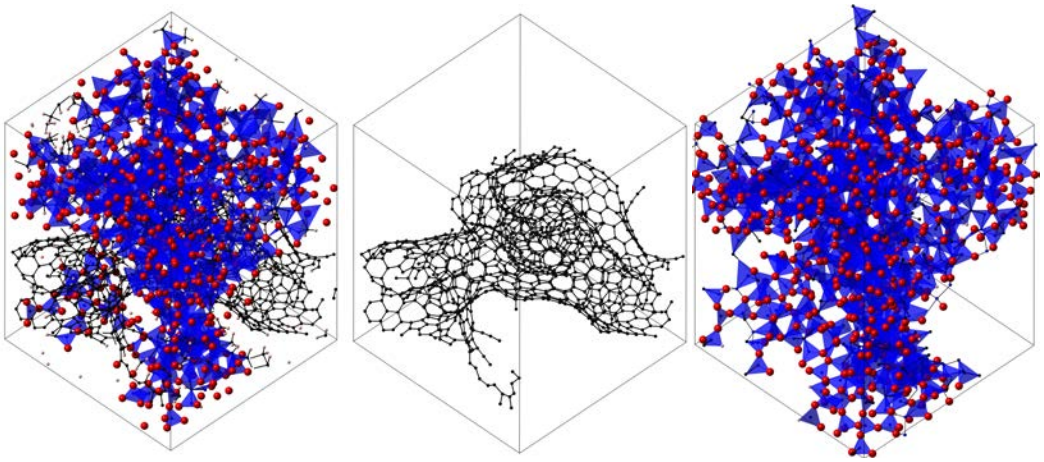

Figure 10. The structure of a-SiCO obtained by simulated annealing of PMHS-DVB polymer precursor: the whole structure (left), free carbon phase (center), and a-SiCO phase (right).

4. Conclusion

We developed new ReaxFF potential parameters for interactions among elements Si, C, O, and H through optimization and learning algorithms. The force field shows excellent agreement with Density Functional Theory calculations for energy differences for a vast variety of compositions and configurations. Moreover, local minima on the potential energy surfaces of both methods agree with each other. The force field demonstrates its predictive capability in simulations of thermal treatment of polysiloxanes. Modeling the polymer-to-ceramic conversion[14] of a cross-linked PHMS/DVB[64] polymer we find remarkable agreement of composition, mass loss, and density of ceramic between experimental data[4, 51, 72-73] and simulation.

The force field enables simulations of fundamental chemical reactions in synthesis and processing of new materials. This encompasses new SiCO ceramic materials, either synthesized by a polymer-to-ceramic route or via the sol-gel process. Preliminary results show successful simulations of condensation reactions for trimethylethoxysilane into a gel-type system. Further applications are reactions occurring during deposition of during low-k dielectric SiCO:H materials, as well as thermal treatment of these materials (post or concurrent synthesis) in reactive atmospheres such as H_2O, CO_2, or H_2. Future direction involve thermodynamic and kinetic stability of dielectric films[74], thermal conductivity[75], and the effects of radiation damage[8, 76] or ion implantation[74]. Obviously, force field development is an ongoing process with room for improvement and progress. Adding additional elements, especially N and B, will broaden the scope of applications. With concurrent computer facilities, it becomes possible to perform simulations of several nanoseconds on the length scale of several nanometers with fidelity comparable to quantum-chemical calculations.

5. Acknowledgements

This work was supported by NSF (CMMI-1634448). Computational work was made possible through generous grants by the Texas Advance Computing Center in Austin, TACC, Texas and UTA HPC facilities.

References

1. Soraru, G. D.; Modena, S.; Guadagnino, E.; Colombo, P.; Egan, J.; Pantano, C., Chemical Durability of Silicon Oxycarbide Glasses. *J Am Ceram Soc* **2002**, *85*, 1529-1536.
2. Rouxel, T.; Massouras, G.; Soraru, G. D., High Temperature Behavior of a Gel-Derived Sioc Glass: Elasticity and Viscosity. *J Sol-Gel Sci Techn* **1999**, *14*, 87-94.
3. Walter, S.; Soraru, G. D.; Brequel, H.; Enzo, S., Microstructural and Mechanical Characterization of Sol Gel-Derived Si-O-C Glasses. *J Eur Ceram Soc* **2002**, *22*, 2389-2400.
4. Soraru, G. D., Kundanati, L., Santhosh, B., Pugno, N., Influence of Free Carbon on the Young's Modulus and Hardness of Polymer‐Derived Silicon Oxycarbide Glasses. *Journal of American Ceramic Society* **2019**, *102*, 907-913.
5. Lee, L. L.; Tsai, D. S., A Hydrogen-Permselective Silicon Oxycarbide Membrane Derived from Polydimethylsilane. *J Am Ceram Soc* **1999**, *82*, 2796-2800.
6. Juttke, Y.; Richter, H.; Voigt, I.; Prasad, R. M.; Bazarjani, M. S.; Gurlo, A.; Riedel, R., Polymer Derived Ceramic Membranes for Gas Separation. *Chem Engineer Trans* **2013**, *32*, 1891-1896.
7. Chiang, C. C.; Ko, I. H.; Chen, M. C.; Wu, Z. C.; Lu, Y. C.; Jang, S. M.; Liang, M. S., Physical and Barrier Properties of Pecvd Amorphous Silicon-Oxycarbide from Trimethylsilane and Co2. *J Electrochem Soc* **2004**, *151*, G704-G708.
8. Ding, H. P.; Demkowicz, M. J., Hydrogen Enhances the Radiation Resistance of Amorphous Silicon Oxycarbides. *Acta Mater* **2017**, *136*, 415-424.
9. Nastasi, M.; Su, Q.; Price, L.; Santana, J. A. C.; Chen, T. Y.; Balerio, R.; Shao, L., Superior Radiation Tolerant Materials: Amorphous Silicon Oxycarbide. *J Nucl Mater* **2015**, *461*, 200-205.
10. Tamayo, A.; Ruiz-Caro, R.; Mazo, A.; Veiga-Ochoa, M. D.; Rubio, J., Chemical Oxidation of Silicon Oxycarbide Ceramics for Advanced Drug Delivery Systems. *J Mater Sci* **2016**, *51*, 1382-1391.
11. Suyal, N.; Krajewski, T.; Mennig, M., Microstructural and Dielectric Characterization of Sol-Gel Derived Silicon Oxycarbide Glass Sheets. *J Sol-Gel Sci Techn* **1999**, *14*, 113-123.
12. David, L.; Bhandavat, R.; Barrera, U.; Singh, G., Silicon Oxycarbide Glass-Graphene Composite Paper Electrode for Long-Cycle Lithium-Ion Batteries. *Nat Commun* **2016**, *7*.
13. Pantano, C. G.; Singh, A. K.; Zhang, H. X., Silicon Oxycarbide Glasses. *J Sol-Gel Sci Techn* **1999**, *14*, 7-25.
14. Colombo, P.; Mera, G.; Riedel, R.; Soraru, G. D., Polymer-Derived Ceramics: 40 Years of Research and Innovation in Advanced Ceramics. *J Am Ceram Soc* **2010**, *93*, 1805-1837.
15. Gallis, S.; Nikas, V.; Huang, M.; Eisenbraun, E.; Kaloyeros, A. E., Comparative Study of the Effects of Thermal Treatment on the Optical Properties of Hydrogenated Amorphous Silicon-Oxycarbide. *J Appl Phys* **2007**, *102*.
16. Rouessac, V.; Favennec, L.; Remiat, B.; Jousseaume, V.; Passernard, G.; Durand, J., Precursor Chemistry for Ulk Cvd. *Microelectron Eng* **2005**, *82*, 333-340.

17. Ryan, J. V.; Pantano, C. G., Synthesis and Characterization of Inorganic Silicon Oxycarbide Glass Thin Films by Reactive Rf-Magnetron Sputtering. *J Vac Sci Technol A* **2007**, *25*, 153-159.
18. Brequel, H., et al., Systematic Structural Characterization of the High-Temperature Behavior of Nearly Stoichiometric Silicon Oxycarbide Glasses. *Chem Mater* **2004**, *16*, 2585-2598.
19. Das, G.; Mariotto, G.; Quaranta, A., Microstructural Evolution of Thermally Treated Low-Dielectric Constant Sioc : H Films Prepared by Pecvd. *J Electrochem Soc* **2006**, *153*, F46-F51.
20. Bois, L.; Maquet, J.; Babonneau, F.; Mutin, H.; Bahloul, D., Structural Characterization of Sol-Gel Derived Oxycarbide Glasses .1. Study of the Pyrolysis Process. *Chem Mater* **1994**, *6*, 796-802.
21. Nimmo, J. P.; Kroll, P., First-Principles Calculations and Analysis of Si-29 Nuclear Magnetic Resonance Chemical Shifts in Silicon Oxycarbide Ceramics. *J Phys Chem C* **2014**, *118*, 29952-29961.
22. Mera, G.; Navrotsky, A.; Sen, S.; Kleebe, H. J.; Riedel, R., Polymer-Derived Sicn and Sioc Ceramics - Structure and Energetics at the Nanoscale. *J Mater Chem A* **2013**, *1*, 3826-3836.
23. Mera, G.; Gallei, M.; Bernard, S.; Ionescu, E., Ceramic Nanocomposites from Tailor-Made Preceramic Polymers. *Nanomaterials-Basel* **2015**, *5*, 468-540.
24. Stabler, C.; Ionescu, E.; Graczyk-Zajac, M.; Gonzalo-Juan, I.; Riedel, R., Silicon Oxycarbide Glasses and Glass-Ceramics: "All-Rounder" Materials for Advanced Structural and Functional Applications. *J Am Ceram Soc* **2018**, *101*, 4817-4856.
25. Kroll, P., Modelling and Simulation of Amorphous Silicon Oxycarbide. *J Mater Chem* **2003**, *13*, 1657-1668.
26. Kroll, P., Searching Insight into the Atomistic Structure of Sico Ceramics. *J Mater Chem* **2010**, *20*, 10528-10534.
27. David Marshall, B. C., Peter Kroll, Greg Hilmas, William Fahrenholtz, Rishi Raj, Robert Ritchie, Qingda Yang, Frank Zok *National Hypersonic Science Center for Materials and Structures*; 2014; p 61.
28. van Duin, A. C. T.; Dasgupta, S.; Lorant, F.; Goddard, W. A., Reaxff: A Reactive Force Field for Hydrocarbons. *J Phys Chem A* **2001**, *105*, 9396-9409.
29. Soria, F. A.; Zhang, W. W.; van Duin, A. C. T.; Patrito, E. M., Thermal Stability of Organic Monolayers Grafted to Si(111): Insights from Reaxff Reactive Molecular Dynamics Simulations. *Acs Appl Mater Inter* **2017**, *9*, 30969-30981.
30. Soria, F. A.; Zhang, W. W.; Paredes-Olivera, P. A.; van Duin, A. C. T.; Patrito, E. M., Si/C/H Reaxff Reactive Potential for Silicon Surfaces Grafted with Organic Molecules. *J Phys Chem C* **2018**, *122*, 23515-23527.
31. Newsome, D. A.; Sengupta, D.; Foroutan, H.; Russo, M. F.; van Duin, A. C. T., Oxidation of Silicon Carbide by O-2 and H2o: A Reaxff Reactive Molecular Dynamics Study, Part I. *J Phys Chem C* **2012**, *116*, 16111-16121.
32. Ding, H. P.; Demkowicz, M. J., Hydrogen Reverses the Clustering Tendency of Carbon in Amorphous Silicon Oxycarbide. *Sci Rep-Uk* **2015**, *5*.
33. Gao, H. F.; Wang, H. J.; Zhao, Z. H.; Niu, M.; Su, L.; Wei, Y., Reactive Dynamics Simulation Study on the Pyrolysis of Polymer Precursors to Generate Amorphous Silicon Oxycarbide Structures. *J Phys Chem C* **2018**, *122*, 5767-5773.

34. Srinivasan, S. G.; van Duin, A. C. T.; Ganesh, P., Development of a Reaxff Potential for Carbon Condensed Phases and Its Application to the Thermal Fragmentation of a Large Fullerene. *J Phys Chem A* **2015**, *119*, 571-580.
35. Bodifort, N. Crystalline Sico: Implication on Structure and Thermochemistry of Ternary Silicon Oxycarbide Ceramics. The University of Texas at Arlington, 2013.
36. Wooten, F.; Winer, K.; Weaire, D., Computer-Generation of Structural Models of Amorphous Si and Ge. *Phys Rev Lett* **1985**, *54*, 1392-1395.
37. Kroll, P., Structure and Reactivity of Amorphous Silicon Nitride Investigated with Density-Functional Methods. *J Non-Cryst Solids* **2001**, *293*, 238-243.
38. Hohenberg, P.; Kohn, W., Inhomogeneous Electron Gas. *Phys Rev B* **1964**, *136*, B864-+.
39. Kresse, G.; Hafner, J., Ab-Initio Molecular-Dynamics Simulation of the Liquid-Metal Amorphous-Semiconductor Transition in Germanium. *Phys Rev B* **1994**, *49*, 14251-14269.
40. Kresse, G.; Furthmuller, J., Efficiency of Ab-Initio Total Energy Calculations for Metals and Semiconductors Using a Plane-Wave Basis Set. *Comp Mater Sci* **1996**, *6*, 15-50.
41. Blochl, P. E., Projector Augmented-Wave Method. *Phys Rev B* **1994**, *50*, 17953-17979.
42. Kresse, G.; Joubert, D., From Ultrasoft Pseudopotentials to the Projector Augmented-Wave Method. *Phys Rev B* **1999**, *59*, 1758-1775.
43. Perdew, J. P.; Burke, K.; Ernzerhof, M., Generalized Gradient Approximation Made Simple. *Phys Rev Lett* **1996**, *77*, 3865-3868.
44. Perdew, J. P.; Burke, K.; Ernzerhof, M., Generalized Gradient Approximation Made Simple (Vol 77, Pg 3865, 1996). *Phys Rev Lett* **1997**, *78*, 1396-1396.
45. Grimme, S., Semiempirical Gga-Type Density Functional Constructed with a Long-Range Dispersion Correction. *J Comput Chem* **2006**, *27*, 1787-1799.
46. Plimpton, S., Fast Parallel Algorithms for Short-Range Molecular-Dynamics. *J Comput Phys* **1995**, *117*, 1-19.
47. Aktulga, H. M.; Fogarty, J. C.; Pandit, S. A.; Grama, A. Y., Parallel Reactive Molecular Dynamics: Numerical Methods and Algorithmic Techniques. *Parallel Comput* **2012**, *38*, 245-259.
48. Bussi, G.; Donadio, D.; Parrinello, M., Canonical Sampling through Velocity Rescaling. *J Chem Phys* **2007**, *126*.
49. Hornetz, B.; Michel, H. J.; Halbritter, J., Arxps Studies of Sio2-Sic Interfaces and Oxidation of 6h Sic Single-Crystal Si-(001) and C-(001)over-Bar Surfaces. *J Mater Res* **1994**, *9*, 3088-3094.
50. Onneby, C.; Pantano, C. G., Silicon Oxycarbide Formation on Sic Surfaces and at the Sic/Sio2 Interface. *J Vac Sci Technol A* **1997**, *15*, 1597-1602.
51. Dibandjo, P.; Dire, S.; Babonneau, F.; Soraru, G. D., Influence of the Polymer Architecture on the High Temperature Behavior of Sico Glasses: A Comparison between Linear- and Cyclic-Derived Precursors. *J Non-Cryst Solids* **2010**, *356*, 132-140.
52. Takamoto, S.; Yamasaki, T.; Ohno, T.; Kaneta, C.; Hatano, A.; Izumi, S., Elucidation of the Atomic-Scale Mechanism of the Anisotropic Oxidation Rate of 4h-

Sic between the (0001) Si-Face and (000(1)over-Bar) C-Face by Using a New Si-O-C Interatomic Potential. *J Appl Phys* **2018**, *123*.
53. Rouxel, T.; Soraru, G. D.; Vicens, J., Creep Viscosity and Stress Relaxation of Gel-Derived Silicon Oxycarbide Glasses. *J Am Ceram Soc* **2001**, *84*, 1052-1058.
54. Shiina, K.; Kumada, M., Thermal Rearrangement of Hexamethyldisilane to Trimethyl(Dimethylsilylmethyl)-Silane. *J Org Chem* **1958**, *23*, 139-139.
55. Radovanovic, E.; Gozzi, M. F.; Goncalves, M. C.; Yoshida, I. V. P., Silicon Oxycarbide Glasses from Silicone Networks. *J Non-Cryst Solids* **1999**, *248*, 37-48.
56. Yu, Y. T.; Wang, B.; Wang, M. Y.; Sant, G.; Bauchy, M., Revisiting Silica with Reaxff: Towards Improved Predictions of Glass Structure and Properties Via Reactive Molecular Dynamics. *J Non-Cryst Solids* **2016**, *443*, 148-154.
57. Pitman, M. C.; van Duin, A. C. T., Dynamics of Confined Reactive Water in Smectite Clay-Zeolite Composites. *J Am Chem Soc* **2012**, *134*, 3042-3053.
58. Tersoff, J., Empirical Interatomic Potential for Silicon with Improved Elastic Properties. *Phys Rev B* **1988**, *38*, 9902-9905.
59. Tersoff, J., Empirical Interatomic Potential for Carbon, with Applications to Amorphous-Carbon. *Phys Rev Lett* **1988**, *61*, 2879-2882.
60. Kroll, P. Computersimulationen Und Röntgennahkantenabsorptionsspektroskopie Von Siliciumnitrid Und Siliciumcarbidnitrid Keramiken. TU Darmstadt, 1996.
61. Munetoh, S.; Motooka, T.; Moriguchi, K.; Shintani, A., Interatomic Potential for Si-O Systems Using Tersoff Parameterization. *Comp Mater Sci* **2007**, *39*, 334-339.
62. Chatgilialoglu, C., Structural and Chemical-Properties of Silyl Radicals. *Chem Rev* **1995**, *95*, 1229-1251.
63. Liao, N. B.; Xue, W.; Zhou, H. M.; Zhang, M., Molecular Dynamics Investigation of Structure and High-Temperature Mechanical Properties of Sibco Ceramics. *J Alloy Compd* **2014**, *610*, 45-49.
64. Blum, Y. D.; MacQueen, D. B.; Kleebe, H. J., Synthesis and Characterization of Carbon-Enriched Silicon Oxycarbides. *J Eur Ceram Soc* **2005**, *25*, 143-149.
65. Lu, K., Porous and High Surface Area Silicon Oxycarbide-Based Materials-a Review. *Mat Sci Eng R* **2015**, *97*, 23-49.
66. Kleebe, H. J.; Blum, Y. D., Sioc Ceramic with High Excess Free Carbon. *J Eur Ceram Soc* **2008**, *28*, 1037-1042.
67. Sasikumar, P. V. W.; Zera, E.; Graczyk-Zajac, M.; Riedel, R.; Soraru, G. D., Structural Design of Polymer-Derived Sioc Ceramic Aerogels for High-Rate Li Ion Storage Applications. *J Am Ceram Soc* **2016**, *99*, 2977-2983.
68. Graczyk-Zajac, M.; Vrankovic, D.; Waleska, P.; Hess, C.; Sasikumar, P. V.; Lauterbach, S.; Kleebe, H. J.; Soraru, G. D., The Li-Storage Capacity of Sioc Glasses with and without Mixed Silicon Oxycarbide Bonds. *J Mater Chem A* **2018**, *6*, 93-103.
69. Liao, N. B.; Zhou, H. M.; Zheng, B. R.; Xue, W., Silicon Oxycarbide-Derived Carbon as Potentia No2 Gas Sensor: A First Principles' Study. *Ieee Electr Device L* **2018**, *39*, 1760-1763.
70. Du, T.; Li, H.; Sant, G.; Bauchy, M., New Insights into the Sol-Gel Condensation of Silica by Reactive Molecular Dynamics Simulations. *J Chem Phys* **2018**, *148*.

71. Soraru, G. D.; Pederiva, L.; Latournerie, M.; Raj, R., Pyrolysis Kinetics for the Conversion of a Polymer into an Amorphous Silicon Oxycarbide Ceramic. *J Am Ceram Soc* **2002**, *85*, 2181-2187.
72. Prandeep, V. S. Study of Silicon Oxycarbide (Sioc) as Anode Materials for Li-Ion Batteries. University of Trento, 2013.
73. Hourlier, D.; Venkatachalam, S.; Ammar, M. R.; Blum, Y., Pyrolytic Conversion of Organopolysiloxanes. *J Anal Appl Pyrol* **2017**, *123*, 296-306.
74. Chen, J. W.; Calvin, J.; Asplund, M.; King, S. W.; Woodfield, B. F.; Navrotsky, A., Heat Capacities, Entropies, and Gibbs Free Energies of Formation of Low-K Amorphous Si(O)Ch Dielectric Films and Implications for Stability During Processing. *J Chem Thermodyn* **2019**, *128*, 320-335.
75. Harikrishna, H.; Lanford, W. A.; King, S. W.; Huxtable, S. T., Thermal Conductivity of Plasma Deposited Amorphous Hydrogenated Boron and Carbon Rich Thin Films. *J Nucl Mater* **2019**, *514*, 154-160.
76. Su, Q.; Wang, T. Y.; Gigax, J.; Shao, L.; Lanford, W. A.; Nastasi, M.; Li, L. Y.; Bhattarai, G.; Paquette, M. M.; King, S. W., Influence of Topological Constraints on Ion Damage Resistance of Amorphous Hydrogenated Silicon Carbide. *Acta Mater* **2019**, *165*, 587-602.